



# A study on coalescence and breakage mechanisms in three different bubble columns

Domenico Colella<sup>a</sup>, Damiano Vinci<sup>a</sup>, Roberto Bagatin<sup>b</sup>, Maurizio Masi<sup>c</sup>,  
Eiman ABu Bakr<sup>a,\*</sup>

<sup>a</sup>DSM Research, P.O. Box 18, 6160 MD Geleen, The Netherlands

<sup>b</sup>EniChem, Corporate R & D Centre, via G. Fauser, 4, 28100 Novara, Italy

<sup>c</sup>Dipartimento di Chimica Fisica Applicata, Politecnico di Milano, via Mancinelli, 7, 20131 Milano, Italy

## Abstract

A study of the interfacial mechanisms focusing on the coalescence and breakage is carried out in the framework of a BRITE-EURAM project named ADMIRE. The main objective of this study is to develop a new methodology to analyse breakage and coalescence phenomena in bubble columns. For this purpose both detailed measurements of the bubble-size distribution and the development of population balance equation (PBE) model were carried out. An elaborate database is established which describes the evolution of the bubble-size distribution in three different columns at EniChem, Politecnico di Milano and DSM. The database contains a unique set of bubble-size distribution measurements: not only the evolution of this distribution as a function of height in the column has been investigated but also the influence of gas superficial velocity and different hydrodynamic configurations have been studied. The distribution curves were obtained by analysing a large amount of bubbles with a measurement based on a new image analysis technique. The experimental measurements showed a consistent trend on the three sites and the influence of the bubble size on breakage and coalescence rates has clearly been observed. Simultaneously, a novel model that describes bubble–bubble interactions was developed. The advantage of this new model with respect to models published in literature is that the physics of free rising bubbles (e.g. wake interactions, bubble swarm velocity and the shape of the bubbles) are also taken into account. Moreover, this model is especially tailored for bubble columns where the physics of the interfacial mechanisms is thought to play a major role. For this reason this model distinguishes itself from general-purpose models which usually describe less accurately the phenomena taking place in such particular systems. The validation of the model using the experimental data is satisfactory. © 1999 Elsevier Science Ltd. All rights reserved.

## 1. Introduction

Gas–liquid contactors are very popular not only in chemical industry, but also in other fields (mining, biochemical, and pharmaceutical, etc.). Mass transfer between the gas and liquid phase usually limits the productivity of these units; therefore, a correct estimation of interfacial area is an essential design criterion.

Bubble size distribution in a vessel is not constant, but may change due to bubble–bubble interactions that can lead to breakage or coalescence. No broadly applicable model for the determination of these two rates has yet been presented due to both the unsatisfactory under-

standing of the physical mechanisms that lead to breakage and coalescence and the enormous difficulty in obtaining reliable data, especially for high gas flow rates. The latter is the reason why bubble-size distributions measurements are not so common in literature, and, often, different techniques lead to different measured values. Moreover, almost all the published data refer to the evaluation of a mean bubble diameter inside the column usually estimated from a one-height measurement.

It can be asserted that almost all the distributions available in literature (see Akita & Yoshida, 1974; Miyahara, Matsuba & Takahashi, 1983; Miyahara & Hayashino, 1995; Miyahara & Tanaka, 1997; Prince & Blanch, 1990) have been obtained by measuring a statistically unsatisfactory number of bubbles (usually about 100–200 bubbles divided in 8–10 classes). Such

\* Corresponding author.

distributions are hardly reliable since the shape of the distribution only becomes stable after an amount of measurements which is 3–5 times larger than those usually reported in literature.

In literature, generally the bubble-size distributions are measured only for one height (see Varley, 1995; Millies & Mewes, 1996; Akita & Yoshida, 1974; Miyahara et al., 1983; Miyahara & Tanaka, 1997; Miyahara & Hayashino, 1995), so they cannot be used for the determination of breakage and coalescence rates. In fact, to have an independent measure of breakage and coalescence rates, it is essential to perform measurements at several heights: in this way breakage and coalescence are the main responsible of the observed variations in the bubble size distribution.

Otake, Nakao and Mitsuhashi (1977) measured bubble size distributions for several distances from the sparger. They proposed coalescence to be the dominant phenomenon only in the region immediately above the sparger whereas the breakage rate was proposed to be constant as a function of height in the column.

Hesketh, Etchells and Russell (1991) measured bubble size distributions in a horizontal pipe for different distances from the nozzle. From their data, it can be deduced that breakage is the dominant phenomenon; in fact, increasing the distance from the gas distributor, the number of small bubbles augments monotonically until a steady state is reached. Mahajan and Narasimhamurty (1974) reported that by increasing the gas flow rate, the distribution is monotonously shifted to smaller classes.

In the last decades interfacial mechanisms, especially breakage and coalescence, have been the subject of detailed studies. In Prince and Blanch (1990), Grienberger (1992) and Lee, Herickson and Glasgow (1987) breakage rate is determined by bubble-eddy collisions. In Hesketh et al. (1991) breakage is proposed to be essentially due to instabilities of the bubbles: all the bubbles bigger than a critical size are subjected to breakage and they break all with the same velocity.

Experimental observations showed that bubble breakage occurs through the formation of a neck that closes two parts of the bubble (see Miyahara, Tsuchiya & Fan, 1991; Prince & Blanch, 1990; Wilkinson, van Schayk, Spronken & van Dierendonck, 1993).

Coalescence is always considered to be a binary process and its rate is usually expressed by the product of a collision frequency and an efficiency. In Prince and Blanch (1990) and Grienberger (1992), collision frequency is considered to be due to the turbulent field and difference in the rise velocity due to buoyancy and the presence of liquid velocity gradients. The criterion to determine coalescence efficiency is that the contact time of the coalescing bubbles should be bigger than the time needed to drain the liquid film between them. On the other hand, in a more recent work, Stewart (1995) observed that

coalescence usually appeared to be instantaneous and the contact time between bubbles was found to be considerably bigger than the time for coalescence process.

Miyahara et al. (1991) observed that the wake can be considered to be responsible for breakage and coalescence. In the experimental observations reported in Stewart (1995), wake-driven collisions appeared to be the only mechanism leading to breakage or coalescence.

Tsuchiya, Ohsaki and Taguchi (1996) studied the break-up of large bubbles (“caps”) and they found that the dominant breakage mechanism is related to the Wake effect.

The added value of this work as compared to literature is the construction of an experimental database that can be used as input for the description of the interfacial mechanisms of gas–liquid systems. For this reason the evolution of bubble size distribution in the column height, the influence of gas superficial velocity and different hydrodynamic configurations have been investigated. The experiments were carried out in different bubble columns (DSM and POLIMI) and airlifts (EniChem), to point out the importance of different hydrodynamics, and its influence on interfacial mechanisms. Furthermore, a physically based model was developed.

## 2. Experimental procedure

The experiments were performed in columns and airlift reactors having different dimensions and layouts in order to guarantee that the conclusions are not dependent on the particular geometry of the vessel. The experiments were carried out in three different vessels located in DSM, Politecnico di Milano (POLIMI) and EniChem. The measurements include the evolution of bubble size distribution in the column height and the influence of the gas superficial velocity. In Table 1 all the values of the gas superficial velocity and the distance from the sparger for each site, where the measurements were taken, are reported. In Table 1 also the values of the gas hold-up where the measurement were carried out are given; the maximum values in Table 1 were the upper limit for accurate image analysis. The measurements were taken using photographic technique and the size of the field of view was nearly  $52 \times 40$  mm with a resolution of approximately 400,000 pixels (horizontal  $752 \times$  vertical 582). The image analysis method was improved and a new software (BIA, Bubble Image Analysis) for image analysis (faster and more accurate) was developed and implemented. The gas–liquid system investigated in all vessels was air bubbles in tap water.

### 2.1. DSM column

The DSM bubble column was made of Plexiglas with a diameter equal to 15.24 cm and a height of 109 cm.

Table 1

A: the distance (cm) from the sparger at which measurements were carried out; B: gas superficial velocity (cm/s); C: gas hold-up (%)

Site	A	B (C)
DSM	12.5	0.21 (2.5)
	27.5	0.41 (3.0)
	42.5	0.59 (3.9)
	57.5	1.13 (5.8)
EniChem	77.5	0.6 (1.13)
	97.5	0.8 (1.59)
	272.5	
POLIMI	37.5	0.75 (2.35)
	97.5	1.5 (4.42)
	137.5	

Bubbles were generated using a perforated plate having 0.1 cm diameter holes, arranged in an equilateral triangle pattern with a pitch equal to 1 cm.

The gas–liquid system was obtained pumping air into stagnant demineralized water.

The measurements were performed using a SONY CCD camera (model AVC-D5CE) and a stroboscopic lamp positioned opposite to the camera on the same axis. The output from the camera was fed into a PC using a MATROX MGA Millennium® graphic card and OPTIMAS 5.2® software by Optimas Corporation. The bubbles in the pictures were measured using Leica Qwin®, a commercial software for image analysis by Leica.

## 2.2. Polimi column and EniChem airlift

In Politecnico di Milano the bubbles were generated in a cylindrical column, made of PVC, having a diameter equal to 6.8 cm. The unaerated liquid height was set to 270 cm; the bubbles were released from a horizontal porous plate with 0.2 mm diameter holes. The EniChem airlift reactor is 505 cm high and its diameter is 48.5 cm. The column has inside a cylindrical downcomer, having 430 cm in height and 20 cm in diameter. The top of the vessel was open and its walls were characterised by an enlargement of the external and internal tube in the uppermost section. The sparger was a ring with 32 holes having 3 mm diameter, put in the external annular region. The measurements of bubble-size distributions were performed in the riser (external annular region). For further information about the reactor geometry see Bagatin, Andrigo, Protto and Wilhelm (1999).

The images were recorded on an S-VHS cassette with a stroboscopic lamp positioned opposite to the camera on the same axis and then, using Adobe Photo Shop®, sequences from the videotape were converted into an

AVI format file. The pictures taken at EniChem and POLIMI have been analysed using BIA.

## 2.3. Image analysis

The technique has been calibrated focussing the camera on an object of known dimensions put in the centre plane of the column (in DSM and Polimi) or of the riser (in EniChem). The quality of the images was enhanced regulating the contrast. During the analysis only the bubbles on focus were taken into consideration by the operator, since the tracing of the bubbles was carried out manually.

The 2-D picture shape of the bubbles were approximated by ellipses whose major and minor axes were automatically computed by the software program used for image analysis. The third dimension was calculated with the assumption that the bubbles are symmetric around the minor axes (the shape looks “disk” like). Subsequently, the diameter of the sphere with the same volume of the measured ellipsoid was computed. It should thereby be noted that the surface area of the ellipsoid and the equivalent sphere are quite different ( $\approx 10\%$ ). This means that when the surface area is computed on the basis of spherical bubbles having equal volume with respect to the ellipsoidal bubbles then the interfacial area is underestimated. The distributions were obtained sorting the equivalent diameters of the bubbles into different classes: the diameter range obtained from the data analysis was discretized into nine uniform classes. In Table 2 the range values for each class and experimental site are reported.

In order to obtain the distribution curves about 500 bubbles for each distribution were analysed, since this is the number of bubbles to be measured in order to establish a statistically stable distribution (see also Miyahara & Hayashino, 1995; Miyahara et al., 1983; Tsouris & Tavlarides, 1994).

The quality of measurements, performed using BIA, has been verified executing two different tests. The first one was the measurements of sets of ellipses having

Table 2  
Discretization in bubble classes for the three different sites

DSM classes (cm)	Polimi classes (cm)	EniChem classes (cm)
A 0–0.2	A1 0–0.04	J 0–0.24
B 0.2–0.3	A2 0.04–0.07	K 0.24–0.45
C 0.3–0.41	A3 0.07–0.1	L 0.45–0.66
D 0.41–0.52	A4 0.1–0.13	M 0.66–0.86
E 0.52–0.63	A5 0.13–0.17	N 0.86–1.07
F 0.63–0.74	A6 0.17–0.2	O 1.07–1.28
G 0.74–0.84	B1 0.2–0.23	P 1.28–1.48
H 0.84–0.95	B2 0.23–0.26	Q 1.48–1.69
I 0.95–1.06	B3 0.26–0.29	R 1.69–1.9

known dimensions: the results showed a really good agreement both for the determination of major and minor axis (error ~ 3%). The second test consisted of the repetition of experimental bubble-size distributions (previously obtained using the commercial software for image analysis Leica Qwin): also in this case a good agreement (within 5%) was obtained.

### 3. Experimental results and discussion

#### 3.1. EniChem airlift and DSM column

As it can be seen from Figs. 1–6, the relative frequency of the small bubbles (classes A, B, C for DSM column; K, L for EniChem airlift) increases monotonically upon an increase of the distance from the sparger and the gas superficial velocity. The big bubbles (class E, F, G for DSM; M, N and P for EniChem) on the other hand show a consistent reduction. Breakage seems to be the dominant phenomenon since the mean diameter of the distribution decreases as a function of increasing height (i.e. in Fig. 2 from 0.44 to 0.35 cm, in Fig. 3 from 0.8 to 0.53 cm). This result is in perfect agreement with Hesketh et al. (1991).

The effect of the gas superficial velocity is clear as well: its increase enhances bubble–bubble interactions (breakage in this case, see also Mahajan & Narasimhamurty, 1974). This can be illustrated from Fig. 5 in which the increase of the gas superficial velocity (from 0.21 to 1.13 cm/s) is seen to cause a decrease in the mean of the distribution (from 0.56 to 0.35 cm). In Fig. 4 it is furthermore seen that at 12.5 cm from the sparger an increase of the gas superficial velocity causes a flattening of the distribution. At 57.5 cm from the sparger (Fig. 5) however, the peak due to the number of small bubbles (class B) gets sharper by increasing the gas flow rate.

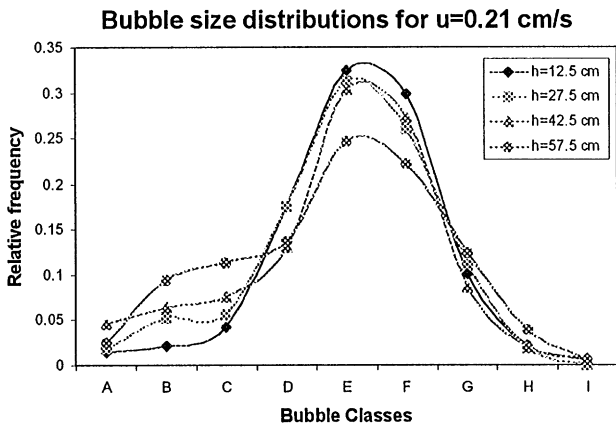


Fig. 1. Relative frequency in DSM column for different heights from the sparger ( $h$ ) at a constant gas superficial velocity  $u = 0.21$  cm/s.

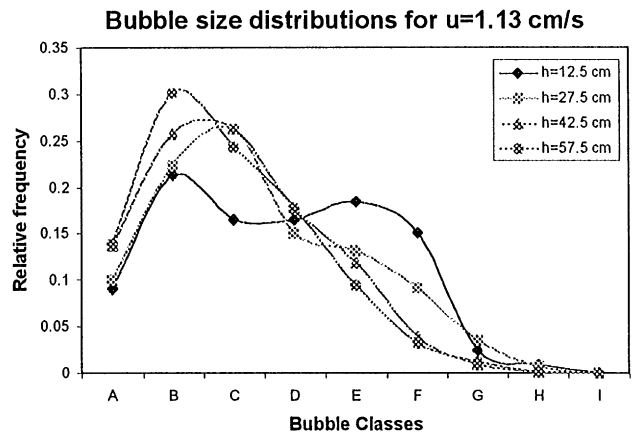


Fig. 2. Relative frequency in DSM column for different heights from the sparger ( $h$ ) at a constant gas superficial velocity  $u = 1.13$  cm/s.

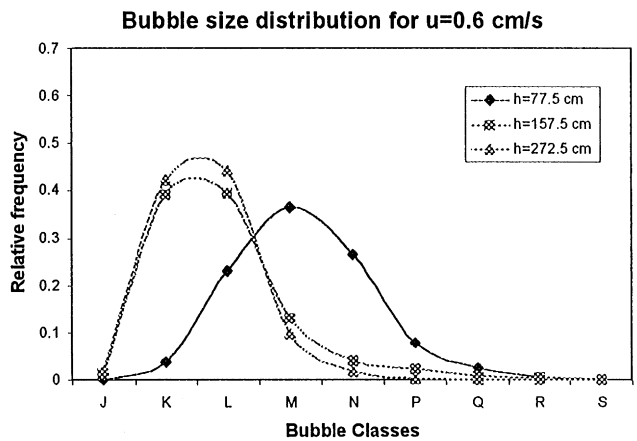


Fig. 3. Relative frequency in EniChem airlift for different heights from the sparger ( $h$ ) at a constant gas superficial velocity  $u = 0.6$  cm/s.

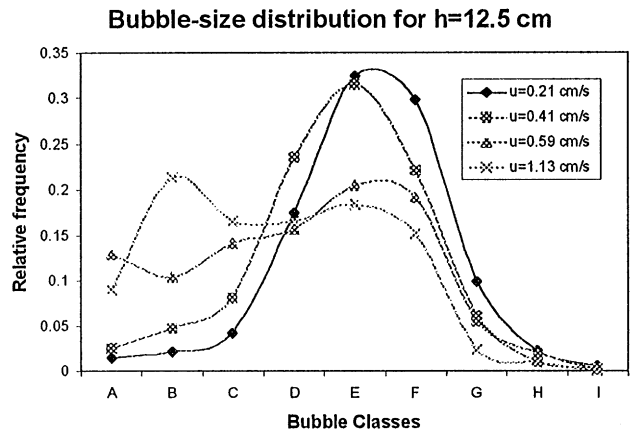


Fig. 4. Relative frequency in DSM column at the constant height of 12.5 cm from the sparger varying the gas superficial velocity ( $u$ ).

#### 3.2. Polimi column

The bubbles in the Polimi bubble column are considerably smaller than those in DSM column: the maximum

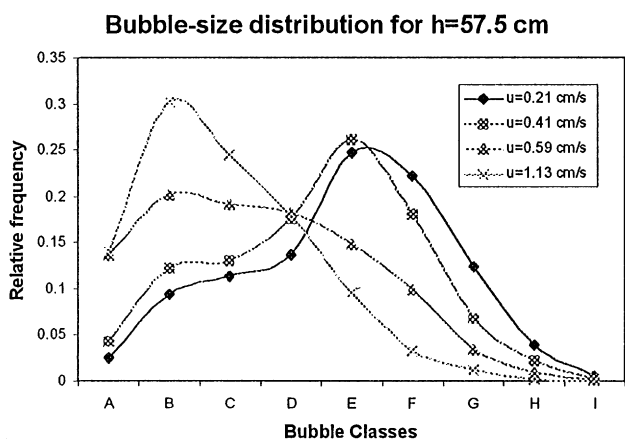


Fig. 5. Relative frequency in DSM column at the constant height of 57.5 cm from the sparger varying the gas superficial velocity ( $u$ ).

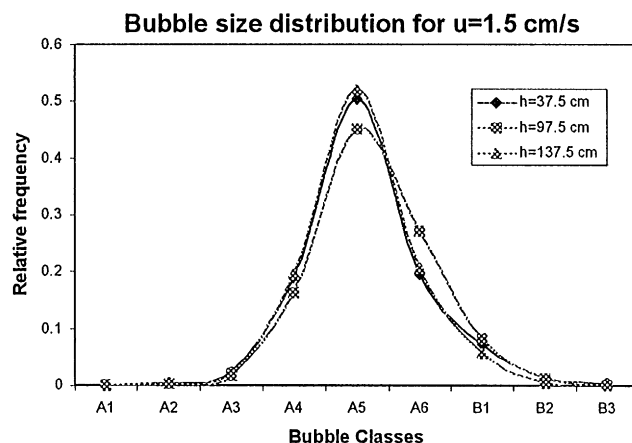


Fig. 7. Relative frequency in Polimi column for different heights from the sparger ( $h$ ), gas superficial velocity  $u = 1.5$  cm/s.

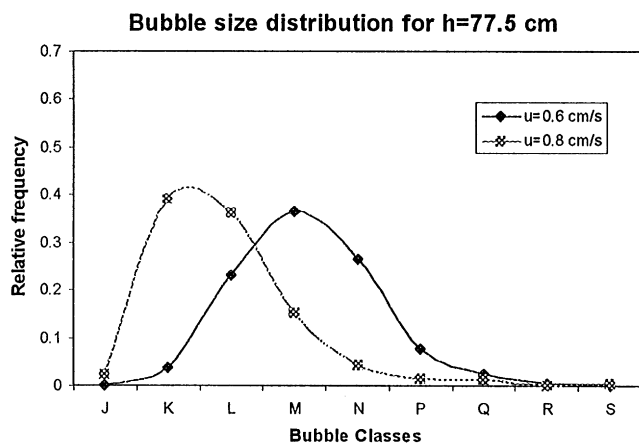


Fig. 6. Relative frequency in EniChem airlift at the constant height of 77.5 cm from the sparger varying the gas superficial velocity ( $u$ ).

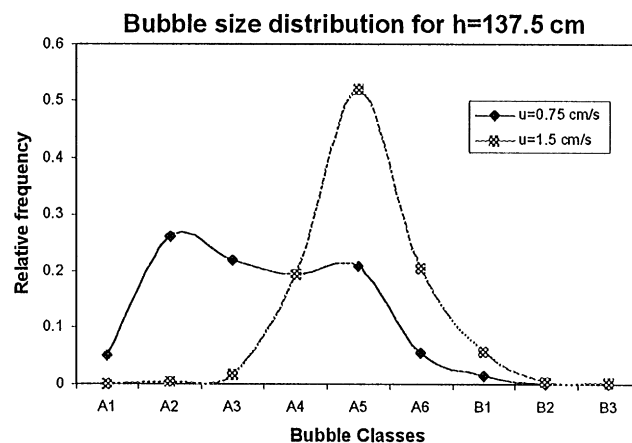


Fig. 8. Relative frequency in Polimi column at the constant height of 137.5 cm from the sparger varying the gas superficial velocity ( $u$ ).

bubble diameter is 0.3 cm (DSM class A and B). In this case, breakage is not the dominant phenomenon (small bubbles do not tend to break) and the measurements showed that the bubble size distribution does not change as a function of column height: already below 37.5 cm from the sparger, equilibrium between breakage and coalescence phenomena is established (see Fig. 7). When gas superficial velocity increases from 0.75 to 1.5 cm/s, there is a shift in the distribution from the small classes to the bigger classes (see Fig. 8). The maximum bubble size remains however small as compared to those from DSM and EniChem. The small size of the bubbles could be due to the sparger that is a porous plate with 0.2 mm diameter holes.

From the overall trend of all distributions from DSM, POLIMI, and EniChem sites the following are concluded:

The measurements in bubble columns (POLIMI, DSM) and airlift reactors (EniChem) show the same

trend. In spite of the presence of a downcomer, the two systems behave in a similar way.

The interactions (breakage and coalescence) between the bubbles are proportional to the gas superficial velocity. Increasing the gas superficial velocity the bubble size distribution changes dramatically. For DSM and EniChem reactors further work (to be published) concerning the sparger zone supports this conclusion: in fact, increasing the gas superficial velocity in the considered range, the bubble size distribution just above the sparger shifts towards the big classes (see also Rabiger & Vogel-pohl, 1983). The influence of hydrostatic pressure (estimated to be  $\sim 3\%$  per meter depth on the bubble diameter of a single rising bubble) can be neglected in the considered columns, as it is comparable to the experimental error.

For constant value of gas superficial velocity, the relative frequency of the bigger bubbles never augments as function of the distance from the gas distributor. Hence,

coalescence rate is less important than breakage rate on the overall height of the column.

The global hydrodynamics of DSM and EniChem columns are quite similar; on the contrary, POLIMI bubble column shows a different trend. This behaviour is thought to be due to the influence of the sparger zone, since at POLIMI a porous plate is used.

The influences of the sparger zone, which is currently investigated (work to be published), play important role in the hydrodynamic of the three columns.

#### 4. Model development

A population balance model provides a statistical formulation to describe the dispersed phase in a multiphase flow. Generally, the population balance equation (PBE) can be expressed by the following equation (see Becker, 1994; Fleischer, Backer & Eigenberger, 1996; Millies & Mewes, 1996):

$$\begin{aligned} & \underbrace{\frac{\partial}{\partial t} f(z, v, t)}_{(i)} + \underbrace{\frac{\partial}{\partial t} [f(z, v, t) u_b(z, v)]}_{(ii)} \\ & + \underbrace{\frac{\partial}{\partial v} \left[ f(z, v, t) \frac{\partial}{\partial t} v_b(z, v) \right]}_{(iii)} \\ & = \underbrace{\frac{\partial}{\partial t} \left[ D_z(z, v) \frac{\partial}{\partial z} f(z, v, t) \right]}_{(iv)} \\ & + \underbrace{B(z, v, t)}_{(v)} + \underbrace{C(z, v, t)}_{(vi)} \end{aligned} \quad (1)$$

where  $f$ ,  $z$ ,  $v$ ,  $t$ ,  $u$  and  $D$  are, respectively, the number density function, the axial coordinate, the bubble volume, the time, the bubble rise velocity and a dispersion coefficient.

The meaning of the terms is:

- i. variation in time
- ii. variation due to bubble transport
- iii. variation due to mass transfer or expansion caused by the decrease of pressure
- iv. dispersion term: this term accounts for mixing effects leading to deviation to axial plug flow
- v. source term due to breakage (particles that break should be eliminated from the population, while the newly formed one should be added)
- vi. source term due to coalescence (for each event two coalescing bubbles are cancelled while the newborn one is added).

It should be remarked that Eq. (1) does not take into account the non-homogeneity of the gas and liquid flow on the radial coordinate.

The term (iv) in Eq. (1) represent an axial dispersion term: its proper definition is not completely clear, but it seems to originate because bubbles move upwards at different velocities or can be driven randomly by the turbulent field (see Deckwer, 1991). Hyndman and Guy (1995) pointed out that the large scatter in dispersion coefficients reported in literature shows that the axial dispersion model is perhaps over-simplified and its use is not recommendable.

A new model based on the physics of bubble columns has been developed within DSM to evaluate breakage and coalescence rates. The novel features introduced in the model are:

- The Wake effect
- The Shape effect

The Wake effect is due to the fact that every bubble rising in a liquid determines the hydrodynamics in a portion of space at its rear. For this reason it is considered to be the driving mechanism for bubble–bubble interactions (see Stewart, 1995; Miyahara et al., 1991).

Concerning the Shape, bubbles rising in a liquid generally cannot be considered as spheres (that holds only for very small bubbles). Their shape can influence both breakage (the crucial step for breakage to occur is the formation of a neck) and coalescence (which determines the amount of liquid between the coalescing bubbles to be drained).

By the introduction of the bubble concentration  $n$ , defined as number of bubbles per unit volume instead of the number density function  $f$ , Eq. (1) can be rearranged using the following hypotheses:

- The bubble volume axis is discretized into  $N$  “classes of bubbles”.
- Mass transfer and expansion due to the decreasing pressure, term (iii) in Eq. (1), are neglected.
- Bubble-rise velocity is only a function of their class and radial position.
- The horizontal component of bubble velocity can be neglected compared to the vertical one.
- Transport on the  $z$ -axis (ii) is considered to be the dominant phenomenon.
- The column is considered to be constituted by a set of  $M$  concentric plug flows, with no exchange between them.

On this basis the PBE can be transformed in a system of  $M \times N$  ordinary differential equations:

$$u_{kr} \frac{\partial n_{kr}(z)}{\partial z} = Br_{kr} + C_{kr}, \quad (2)$$

where  $k = 1, 2, \dots, N$  and  $r = 1, 2, \dots, M$  are subscripts referring, respectively, to the bubble classes and to the radial grid.

Considering that breakage, and not only coalescence, is due to binary interactions with other bubbles and leads to the formation of two daughter-bubbles, Eq. (2) can be written as

$$\begin{aligned}
 \underbrace{u_{kr} \cdot \frac{\partial n_{kr}(z)}{\partial z}}_{\text{bubble-transport}} &= \underbrace{\frac{1}{2} \sum_{i,j} c_{ijk} H_{ijr} \lambda_{ij}}_{\text{birth-due-to-coalescence}} \\
 &- \underbrace{\sum_i H_{ikr} \lambda_{ik}}_{\text{death-due-to-coalescence}} + \underbrace{\frac{1}{2} \sum_{i,j>k} \beta_{jk} H_{ij} \eta_{ij}}_{\text{birth-due-to-breakage}} \\
 &- \underbrace{\sum_i H_{ikr} \eta_{ik}}_{\text{death-due-to-breakage}}
 \end{aligned} \quad (3)$$

where  $i, j, k = 1, 2, \dots, N$  and  $r = 1, 2, \dots, M$  are subscripts referring, respectively, to the bubble classes and the radial grid;  $u, n, H, \lambda, \eta$  are, respectively, bubble rise velocity, concentration of bubbles belonging to  $k$ th class, collision frequency, coalescence and breakage efficiency;  $c_{ijk}$  states if the coalescence of a bubble  $i$  with one of class  $j$  leads to the formation of a bubble of the  $k$ th class;  $\beta_{jk}$  is the amount of bubbles belonging to class  $k$  formed from the rupture of one of the  $j$ th class.

Concerning daughter-bubble distribution, small bubbles (up to 0.3 cm) are considered to break in equal size daughters, the bigger ones are considered not to break in a preferential size range.

## 5. Evaluation of breakage and coalescence rates

Several models in literature (mentioned in the introduction) are affected by hypotheses that are not suitable in the case of free rising bubbles:

- Gas kinetic theory is used to calculate collision frequency between bubbles: this approach considers bubbles interacting only during collision, and neglects that they influence each other by means of their wakes.
- Breakage efficiency is not affected by the shape. In reality the shape of a bubble can affect sensibly breakage, because the flatter is the bubble, the easier is to form necks.
- Coalescence time is usually one order of magnitude smaller than contact time; hence, the probabilistic hypotheses used for the calculation of coalescence efficiency are not valid.

Hereby it is assumed that the wake is the driving mechanism for bubble–bubble interactions. It can be remarked that the introduction of the wake implies the rise of a non-symmetric configuration. Therefore, in the following part the first subscript ( $i$ ) refers to the leading bubble, the second ( $j$ ) to the trailing one and  $r$  to the node on the

radial grid (i.e.  $x_{ijr}$  refers to the configuration  $i$  leading,  $j$  trailing on the  $r$ th node on the radial grid).

### 5.1. Evaluation of bubble shape

The bubbles will be considered to be oblate ellipsoids: the ratio between major ( $a$ ) and minor axes ( $b$ ) can be expressed as a function of Eötvös number (see Clift, Grace & Weber, 1978)

$$s = a/b = 1 + 0.163 \cdot \text{Eö}^{0.757}. \quad (4)$$

### 5.2. Evaluation of bubble swarm velocity

Miyahara and Fan (1992) observed that the rising velocity of a large bubble in a bubble swarm relative to the liquid is extremely high compared to that of single bubbles: they assumed the increase to be due to the wake of leading bubbles. The rise velocity of in-line bubbles can be estimated from the terminal velocity of the isolated bubbles plus a term accounting for the extra-speed due to the wake.

In first approximation the bubble velocity in a column can be considered dependent only on the radial position. Using Richardson and Zucki (1954) equation, the local bubble velocity can be written as

$$u_{(\phi)} = u_b [1 - \varepsilon(\phi)]^{m-1} + u_l(\phi), \quad (5)$$

where  $u, u_b, u_l, \varepsilon$  are, respectively, the local bubble velocity, the terminal rise velocity, the local liquid velocity and the gas hold-up;  $\phi$  is the dimensionless radial coordinate and  $m$  is a parameter (see Dobby & Finch, 1986; Dobby, Yanatos & Finch, 1988).

The terminal bubble rise velocity was evaluated by the model of Jamialahmadi and co-workers (see Jamialahmadi, Branch & Müller-Steinhagen, 1994).

The expression for liquid velocity, under the assumption of a step profile of the gas hold-up (in the radial direction) is illustrated in Burns and Rice (1997): the column is divided in three regions where a constant hold-up is assumed.

### 5.3. Wake effect and collision frequency

The proposed equation for collision frequency is

$$H_{ijr} = n_{ir} n_{jr} u_{ij}^{rel} \frac{V_i^{BOX}}{\langle d \rangle}, \quad (6)$$

where  $V_i^{BOX}$  is the volume influenced by the wake of a bubble belonging to class  $i$ ,  $u_{ij}^{rel}$  is the relative velocity between the two colliding bubbles and  $\langle d \rangle$  is the average distance between bubbles in the considered system. The ratio on the right-hand side of Eq. (6) expresses the probability of a bubble to be in the wake of another one.

For the determination of  $V^{BOX}$  and the relative velocity between bubbles Nevers and Wut (1971) model has been used: the wake is considered to be a cone (see Fig. 9) whose base is the cross-sectional area of the bubble. Its height was concluded, on the basis of experimental results (see Nevers & Wut, 1971, Stewart, 1995; Miyahara et al., 1991), to be equal to 5 major axis.

5.4. Breakage efficiency

Considering a bubble on the edge of another one's wake (see Fig. 10), it tends to be sucked into the wake region and there is a net gas flux towards the part of the bubble in the wake. The pressure drop due to the establishment of a gas flow towards the in-wake region can lead to breakage.

Using Bernoulli's theorem and mass conservation the liquid outside the bubble, in region (1), is strangling the neck at a speed ( $u_L$ ) given by

$$u_L = \sqrt{\frac{\rho_g}{\rho_L} \left(\frac{r_2}{r_1}\right)^2} u_{g2}, \tag{7}$$

where  $r_1$  and  $r_2$  are the bubble radius in Sections 1 and 2 (see Fig. 10).

Assuming:

$$u_{g2} \propto \Delta u_L \approx u_{wake}, \tag{8}$$

$$\frac{r_2}{r_1} \propto s - 1, \tag{9}$$

where  $\Delta u_L$  is the liquid velocity variation due to the wake; the parameter  $s$  is defined by Eq. (4). Eq. (9) is obtained imposing that very small bubbles should not be affected by breakage.

The breakage efficiency  $\eta_{ij}$  can be considered proportional to  $u_L$ :

$$\eta_{i,j} = k_1 \sqrt{\frac{\rho_g}{\rho_L}} \cdot u_{wake,i} (s_j - 1)^2 \tag{10}$$

where the constant  $k_1$  is considered to be an adjustable parameter.

It is worth to remark that Eq. (10) gives a dependence from gas density in agreement with the experimental data reported in Wilkinson et al. (1993).

5.5. Coalescence efficiency

Two approaching bubbles, as sketched in Fig. 11, are considered: the origin of the coordinate system is on the leading bubble and the trailing bubble is approaching with velocity  $u_{rel}$ . The following assumptions are now made:

- The liquid is an incompressible, non-viscous fluid.
- There are free-slip conditions on the interface; hence the velocity profile in the film is flat.

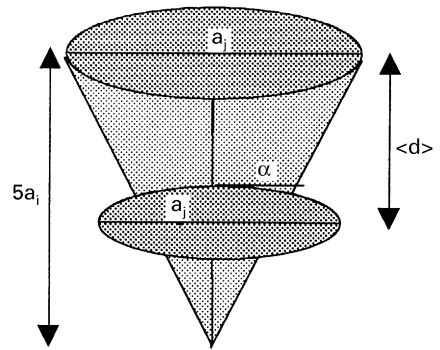


Fig. 9. Sketch of the geometric approximations used for the wake model.

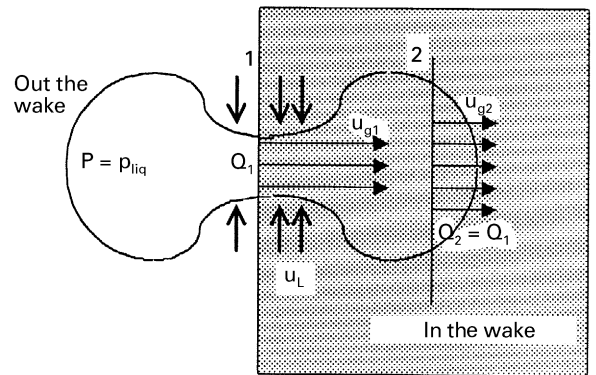


Fig. 10. Sketch of a breaking bubble;  $Q_i$  is the flow rate and the subscripts 1 and 2 refers to the sections.

- The approaching interfaces are and remain flat.
- The volume of the liquid film can be approximated by a cylinder, with base a circle having radius  $R$ , and height  $h$ .
- Every bubble carries with it a mass of fluid equal to  $m \approx \rho_L V/2$  (virtual or added mass).
- Axial and tangential velocity in the liquid film are negligible compared to the radial one.

Using the mass conservation the following radial velocity profile can be found (for the symbols refer to Fig. 11)

$$u_r(r) = \frac{r}{2h} \frac{dh}{dt} = \frac{r}{2h} h'. \tag{11}$$

By using Bernoulli's theorem and Eq. (11), it is possible to calculate the pressure at a distance  $r$  from the centre. If it is furthermore assumed that the value of the integral of the pressure on the circle is equal to the inertial force of the trailing bubble, the following equation is obtained:

$$\begin{aligned} -mh'' &= \int_0^R P 2\pi r dr \\ &= \pi R^2 P_{int} - \frac{1}{2} \rho_L \int_0^R \left(\frac{r}{2h} h'\right)^2 2\pi r dr, \end{aligned} \tag{12}$$

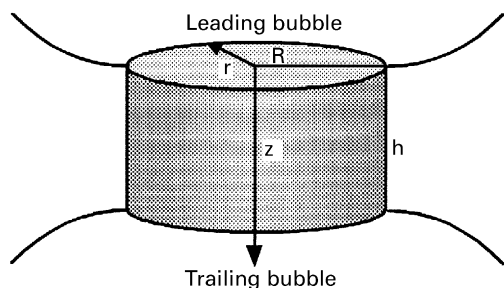


Fig. 11. Sketch of two coalescing bubbles.

where  $P_{int}$  is the pressure in the centre (there liquid velocity is 0).

Bernoulli theorem between the centre and the edge ( $P = 0$ ) of the circle lead to

$$P_{int} = \frac{1}{2}\rho_L u_r^2(R). \tag{13}$$

Substituting Eq. (13) into Eq. (12), the differential equation (14) with the boundary conditions (15) is obtained

$$h'' = -\frac{\pi}{16} \frac{\rho_L R^4}{m} \left(\frac{h'}{h}\right)^2, \tag{14}$$

$$h(0) = h_0,$$

$$h'(0) = u_{rel}. \tag{15}$$

The average draining velocity, can be expressed as

$$\bar{h}' = h'(\bar{t}) = h'(k\tau) = h'(0) + h''(0)k_2\tau, \tag{16}$$

where  $\tau$  is the time required to drain the film and  $k_2$  is an adjustable parameter.

The coalescence efficiency  $\lambda$  can be considered to be proportional to the average drain velocity, using a proportionality constant  $c$ : imposing that for  $d \rightarrow 0$ ,  $\lambda \rightarrow 1$  (see Duineveld, 1994) then  $c = 1/u_{rel}$ .

The discrete form obtained by introducing bubble classes is reported below.

$$\lambda_{ij} = 1 - k_2 \frac{\pi}{16} \frac{\tau u_{ij}^{rel} R_{ij}^4}{v_j h_{0,ij}^2}. \tag{17}$$

It is important to point out that expression (17) is coherent with the experimental observations made by Stewart (1995) and Duineveld (1994): increasing  $u_{rel}$  bubbles tends to bounce apart.

For the determination of the radius of the film to drain ( $R_{ij}$ ) and its initial thickness ( $h_{0,ij}$ ) the following approximation are used (see Patlazhan & Lindt, 1996):

$$r_{ij} \propto \frac{d_i d_j}{d_i + d_j}, \quad R_{ij} \propto r_{ij}^3, \quad h_{0,ij} \propto \frac{3\mu_L(u_{t,i} + 0.5u_{ij}^{rel})}{2\sigma} R_{ij}, \tag{18}$$

where  $d$  is the bubble diameter,  $\sigma$  is the interfacial tension and  $\mu_L$  is liquid viscosity.

### 6. Model validation

The model is validated using the experimental data presented in this article.

The presented model does not include the modelling of the sparger, as it was developed focusing on the determination of breakage and coalescence rates. Hence, the measurement at the lower height was used as the initial condition for the computation of the other ones.

The adjustable parameters of the model were tuned using only one set of data (e.g. DSM measurements). The obtained values for the adjustable parameters were:  $\langle d \rangle = 1$  (see Eq. (6)),  $k_1 = 12.5$  (see Eq. (10)),  $k_2 = 12$  (see Eq. (17)), when c.g.s. System is adopted.

The discretization into bubble classes is given in Table 2.

From Figs. 12 and 13 it is seen that the accuracy of the model is good not only for DSM column, but also for totally different experimental set-up (for vessel dimensions and hydrodynamics) such as the Polimi and

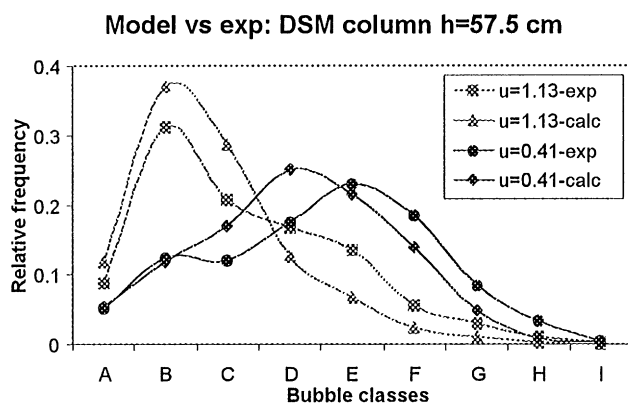


Fig. 12. Comparison of calculated and measured relative frequency for DSM column at 57.5 cm from the sparger and gas superficial velocity set to 1.13 and 0.41 cm/s.

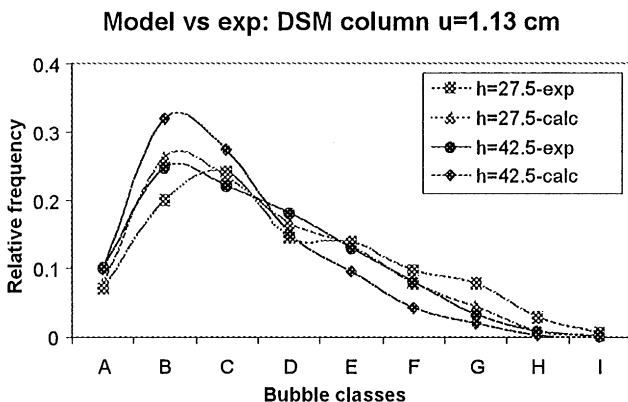


Fig. 13. Comparison of calculated and measured relative frequency for DSM column; gas superficial velocity set to 1.13 cm/s at 42.5 and 27.5 cm from the sparger.

### Model vs exp: Polimi column $u=1.5$ cm

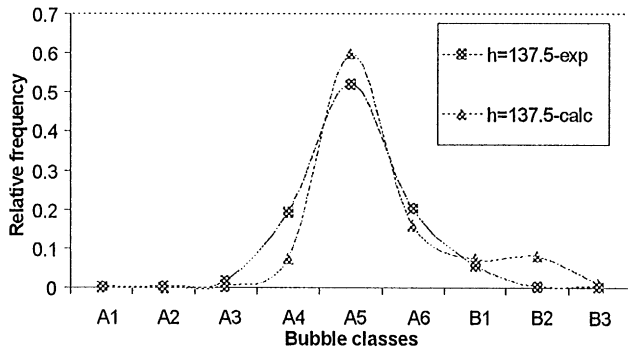


Fig. 14. Comparison of calculated and measured relative frequency for Polimi column at 137.5 cm from the sparger; gas superficial velocity set to 1.5 cm/s.

### Model vs exp: Enichem airlift

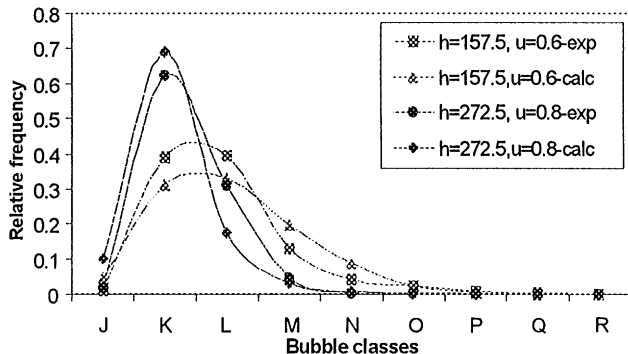


Fig. 15. Comparison of calculated and measured relative frequency for EniChem airlift.

EniChem columns (see Figs. 14 and 15). It is worth to remark that the curves obtained for EniChem and Polimi data are predictions since no further adjustment for the parameters was made. Their satisfactory agreement is the proof of the good quality of the proposed model. Moreover, the trend shown by the prediction, both increasing the height and the gas flow rate, is the same found in the experiments.

## 7. Conclusions

To understand the interfacial mechanisms of gas–liquid reactors (bubble columns), which play an important role in the reactor performance, detailed sets of data of bubble size distribution were investigated. The bubble size distribution measurements were carried out at different bubble columns (DSM and Politecnico di Milano) and airlifts (EniChem). In order to obtain the distribution curves about 500 bubbles for each distribution were analysed.

The measurements were taken using photographic technique.

The evolution of bubble size distribution in the column height and the influence of the gas superficial velocity were pointed out.

The image analysis method was improved and a new software (BIA) for image analysis (faster and more accurate) was developed and implemented.

Furthermore, a new model has been developed which describes bubble–bubble interactions to obtain a reliable evaluation of breakage and coalescence rates in bubble columns.

The advantage of the developed model for bubble columns with respect to those published in literature is that the physics of free rising bubbles (e.g. wake interactions, bubble swarm velocity and the shape of the bubbles) were taken into account.

The rates calculated using the proposed model have been used in the population balance equation to determine the evolution of bubble-size distribution inside bubble columns.

The satisfactory agreement between model predictions and experimental data obtained in three different vessels (two bubble columns in DSM and Polimi and one airlift in EniChem) confirms the reliability of the model to simulate the evolution of bubble size distribution in gas–liquid contactors.

## Notation

$B$	source term due to breakage
$C$	source term due to coalescence
$d$	bubble diameter
$\langle d \rangle$	average distance between bubbles
$f$	number density function
$H$	collision frequency
$h$	thickness of the film to drain
$h_0$	initial thickness of the film
$m$	virtual mass of a bubble
$M$	number of nodes on the radial grid
$n$	bubble concentration
$N$	number of bubble classes
$P_{\text{int}}$	pressure in the centre of the liquid film
$r$	radial coordinate
$R$	radius of the film to drain
$s$	ratio major/minor axis of the bubble
$t$	time
$u$	velocity
$u_t$	bubble terminal rise velocity
$u^{\text{rel}}$	relative velocity
$v$	bubble volume
$V^{\text{BOX}}$	volume of liquid influenced by the wake
$z$	axial coordinate
$\Delta u_L$	gradient of liquid velocity across the wake

## Greek letters

$\varepsilon$	gas hold-up
$\eta$	breakage efficiency
$\lambda$	coalescence efficiency
$\mu_L$	liquid viscosity
$\rho_g$	gas density
$\rho_L$	liquid density
$\sigma$	interfacial tension

## Subscripts and superscripts

$i, j, k$	generic bubble classes
$r$	node on the radial grid
$L$	liquid phase
$g$	gas phase
$b$	bubble
1, 2	sections as sketched on the figures

## Acknowledgements

The authors wish to thank the European Commission for their financial support.

## References

- Akita, K., & Yoshida, F. (1974). Bubble size, interfacial area and liquid-phase mass transfer coefficient in bubble columns. *Industrial and Engineering Chemistry*, *13*, 84–91.
- Bagatin, R., Andriago, P., Protto, L., Wilhelm, C. (1999). Internal-loop airlift reactor hydrodynamic study. *Chemical Engineering Science*, submitted for publication.
- Becker, C. (1994). Modellbildung und Simulation von Blasengrößenverteilungen in örtlich verteilten Gas-Flüssigkeitsdispersionen mit Hilfe von Populationsbilanzen. Graduation Thesis, University of Stuttgart.
- Burns, L. F., Rice, R. G. (1997). Circulation in bubble columns. *A.I.Ch.E. Journal* *43*(6), 1390.
- Clift, R., Grace, J. R., & Weber, M. E. (1978). Bubbles, Drops and Particles. New York: Academic Press.
- Deckwer, W. D. (1991). Bubble column reactors. New York: Wiley.
- Dobby, G. S., & Finch, J. A. (1986). Particle collection in columns-gas rate and bubble size effect. *Canadian Metallurgical Quarterly*, *25*, 9.
- Dobby, G. S., Yanatos, J. B., & Finch, J. A. (1988). Estimation of bubble diameter in flotation columns from drift flux analysis. *Canadian Metallurgical Quarterly*, *27*, 85.
- Duineveld, P. C. (1994). Bouncing and coalescence of two bubbles in water. Dissertation, Twente University.
- Fleischer, C., Becker, S., & Eigenberger, G. (1996). Detailed modelling of the chemisorption of CO<sub>2</sub> into NaOH in a bubble column. *Chemical Engineering Science*, *51*, 1715–1724.
- Grienberger, J. (1992). *Untersuchung und Modellierung von Blasensäulen*. Thesis, University of Erlangen-Nuremberg.
- Hesketh, R. P., Etchells, A. W., & Russel, T. W. F. (1991). Bubble breakage in pipeline flow. *Chemical Engineering Science*, *46*, 1.
- Hyndman, C. L., & Guy, C. (1995). Gas phase flow in bubble columns: A convective phenomenon. *Canadian Journal of Chemical Engineering*, *73*, 426–434.
- Jamialahmadi, M., Branch, C., & Müller-Steinhagen, H. (1994). Terminal bubble rise velocity in liquids. *Transactions of Industrial Chemistry Series E, A*, *72*, 119–122.
- Lee, C. -H., Herickson, L. E., & Glasgow, L. A. (1987). Bubble break-up and coalescence in turbulent gas-liquid dispersion. *Chemical Engineering Communication*, *59*, 65–84.
- Mahajan, S. P., & Narashimhamurty, G. S. R. (1974). Size, size distribution & interfacial area for gas-liquid dispersion formed on perforated plates. *Indian Journal of Technology*, *13*, 541–547.
- Millies, M., & Mewes, D. (1996). Phasengrenzflächen in Blasenströmungen — Teil 1: Blasensäulen. *Chemie Ingenieur Technik*, *68*, 660–669.
- Miyahara, T. & Fan L.-S. (1992). Properties of a large bubble in a bubble swarm in a three-phase fluidized bed. *Journal of Chemical Engineering of Japan*, *25*, 278–382.
- Miyahara, T., & Hayashino, T. (1995). Size of bubbles generated from perforated plates in non-Newtonian liquids. *Journal of Chemical Engineering of Japan*, *28*, 596–600.
- Miyahara, T., Matsuba, Y., & Takahashi, T. (1983). The size of bubbles generated from perforated plates. *International Journal of Chemical Engineering*, *23*, 517–523.
- Miyahara, T., & Tanaka, A. (1997). Size of bubbles generated from porous plates. *Journal of Chemical Engineering Japan*, *30*, 335–355.
- Miyahara, T., Tsuchiya, K., & Fan, L. -S. (1991). Effect of turbulent wake on bubble-bubble interactions in a gas-liquid-solid fluidized bed. *Chemical Engineering Science*, *46*, 2368–2373.
- Nevers, N., & Wut, J. -L. (1971). Bubble coalescence in viscous fluids. *A.I.Ch.E. Journal*, *17*, 182–186.
- Otake, T., Tone, S., Nakao, K., & Mitsuhashi, Y. (1977). Coalescence and break-up of bubbles in liquids. *Chemical Engineering Science*, *32*, 377–383.
- Patlazhan, S. A., & Lindt, J. T. (1996). Kinetics of structure development in liquid-liquid dispersions under simple shear flow theory. *Journal of Rheology*, *40*, 1113–1995.
- Prince, M. J., & Blanch, H. W. (1990). Bubble coalescence and break-up in air-sparged bubble columns. *A.I.Ch.E. Journal*, *36*, 1485–1499.
- Rabiger, N., & Vogelpohl, A. (1983). Calculation of bubble size in the bubble and jet regimes for stagnant and flowing Newtonian liquids. *German Journal of Chemical Engineering*, *6*, 173–182.
- Richardson, J. F. & Zaki W. M. (1954). Sedimentation and fluidization, Part I. *Transactions of the Institution of Chemical Engineers*, *32*(6), 35–53.
- Stewart, C. W. (1995). Bubble interaction in low-viscosity liquids. *International Journal of Multiphase Flow*, *21*, 1037–1046.
- Tsouris, C., & Tavlarides, L. L. (1994). Breakage and coalescence models for drops in turbulent dispersion. *A.I.Ch.E. Journal*, *40*, 395–406.
- Tsuchiya, K., Ohsaki, K., & Taguchi, K. (1996). Large and small bubble interaction patterns in a bubble column. *International Journal of Multiphase Flow*, *22*, 121–132.
- Varley, J. (1995). Submerged gas-liquid jets: bubble size prediction. *Chemical Engineering Science*, *50*, 901–905.
- Wilkinson P. M., van Schayk, A., Spronken J. P. M. & van Dierendonck, L. L. (1993). The influence of gas density and liquid properties on bubble break-up. *Chemical Engineering Science* *48*, 1213.